Electrical Models of Excitation-Contraction Coupling and Charge Movement in Skeletal Muscle

R. T. MATHIAS, R. A. LEVIS, and R. S. EISENBERG

From the Department of Physiology, Rush University, Chicago, Illinois 60612

ABSTRACT The consequences of ionic current flow from the T system to the sarcoplasmic reticulum (SR) of skeletal muscle are examined. The Appendix analyzes a simple model in which the conductance g_x, linking T system and SR, is in series with a parallel resistor and capacitor having fixed values. The conductance g_x is supposed to increase rapidly with depolarization and to decrease slowly with repolarization. Nonlinear transient currents computed from this model have some of the properties of gating currents produced by intramembrane charge movement. In particular, the integral of the transient current upon depolarization approximates that upon repolarization. Thus, equality of nonlinear charge movement can occur without intramembrane charge movement. A more complicated model is used in the text to fit the structure of skeletal muscle and other properties of its charge movement. Rectification is introduced into g_x and the membrane conductance of the terminal cisternae to give asymmetry in the time-course of the transient currents and saturation in the curve relating charge movement to depolarization, respectively. The more complex model fits experimental data quite well if the longitudinal tubules of the sarcoplasmic reticulum are isolated from the terminal cisternae by a substantial resistance and if calcium release from the terminal cisternae is, for the most part, electrically silent. Specific experimental tests of the model are proposed, and the implications for excitation-contraction coupling are discussed.

The steps by which a voltage change across the surface membrane initiates contraction in skeletal muscle include many unknowns. These unknowns persist despite the large body of experimental information describing the structural, electrical, and mechanical aspects of excitation and contraction (Costantin, 1975; Endo, 1977; Caputo, 1978; Lüttgau and Moisescu, 1978).

The step that links a voltage change across the membrane of the T system to the release of calcium ions from their internal store in the sarcoplasmic reticulum (SR) is not understood, even though the experimental evidence available is extensive, and only a few mechanisms seem possible.

Three types of mechanism were considered soon after discovery of the T system, the SR, and the T-SR junction: Peachey and Porter (1959), elaborated in Birks (1965), Freygang (1965), and Peachey (1965 *a*, p. 228–230), suggested that ionic current might flow from T system to SR, spreading the membrane potential change into the SR much as an action potential is spread down the

J. GEN. PHYSIOL. © The Rockefeller University Press · 0022-1295/80/07/0001/31 $1.00 1
Volume 76 July 1980 1–31

length of a muscle fiber. Ford and Podolsky (1972), following the lead of Bianchi and Shanes (1959), postulated that a small amount of calcium might cross from the tubular lumen into the gap between T system and SR, the calcium being a transmitter that triggers massive calcium release from the SR. Hodgkin and Horowicz (1960), and then Adrian et al. (1969), suggested that a change in potential across the T-system membrane might release an activator substance, which, in turn, would induce calcium release.

The activator hypothesis has received much attention. It has been expanded by Schneider and Chandler (1973) and by Chandler et al. (1976 *b*) into a model that includes the properties of nonlinear charge movement. The model supposes that the movement of a charged macromolecule embedded in the T-system membrane controls the opening of a calcium channel in the SR some 20 nm distant. The mechanism of coupling between charge movement and calcium release emphasized in the model (Chandler et al., 1976 *b*; Fig. 11) is simple mechanical coupling. A "rigid rod" is supposed to link the motion of a voltage sensor in the T-system membrane to the motion of a gate, which controls the flow of calcium through a channel in the SR membrane. The voltage-sensing charged macromolecule and rigid rod serve as the activator molecule originally proposed by Hodgkin and Horowicz (1960): the rigid rod allows the calcium channel of the SR to be remotely controlled by the voltage sensor in the T-system membrane.

There is some structural evidence consistent with the rigid rod hypothesis. Bridges or pillars connecting T system and SR, suggested by Porter and Franzini-Armstrong (1965, p. 77), have now been seen by Somlyo (1979), B. Eisenberg and Gilai (1979), and B. Eisenberg et al., (1979). (See also Figs. 11 and 12 of Kelly and Kuda, 1979.) But the structural evidence does not provide strong support for a mechanical link between T system and SR. One can just as well suppose that other mechanisms (such as chemical diffusion; see Chandler et al., 1976 *b*, p. 314) provide the action at a distance required to remotely control calcium release.

An important feature of all models invoking remote control is that a change in potential across the SR membrane is not the cause of calcium release. A change in that potential might well be induced by calcium release, but calcium release occurs in these models even if the potential across the SR membranes is held at its resting value.

There is some reason to disbelieve each of the above hypotheses, and little direct evidence for any of them. The trigger calcium hypothesis appears incompatible with experimental data on the effects of extracellular calcium (e.g., Spiecker et al., 1979; Lüttgau and Spiecker, 1979). The "remote control" hypothesis describes a great deal of data; but it is a novel mechanism without precedent in other tissues. Furthermore, remote control models need modification if the normal mechanism of calcium release is similar to that found in skinned fibers (Endo, 1977), namely, if normal release is the result of a change in SR potential.

The hypothesis of electrical coupling has been discounted (Peachey, 1968; Franzini-Armstrong, 1970, 1971, and 1974) for a number of reasons:

(*a*) The junction between the T system and SR is impermeable to molecules visible in the electron microscope.
(*b*) The structure of the junction between T system and SR was thought to consist of diffuse material (feet), bearing no resemblance to the structure of the gap junctions, which are likely to be the path for current flow between electrically coupled cells. This objection is weakened by the recent observation of electron-lucent pillars connecting T system and SR, mentioned just above.
(*c*) The effective capacitance of resting muscle fibers is much smaller than the contribution usually expected from the membranes of the SR. Conversely, it has been thought that the capacitance of the SR membranes would severely "load" the action potential, drastically reducing its rate of rise and conduction velocity.
(*d*) It has been supposed that the potential change within the SR produced by current flow from the T system would necessarily be too small to trigger calcium release. Some have thought that amplification of SR potentials by changes in ionic conductances would produce an "all-or-none" release of calcium, in conflict with the experimental finding that the contraction of a single myofibril is graded by T-system potential (Costantin and Taylor, 1973; Costantin, 1975, p. 212).
(*e*) Current flow into the SR has been considered an unlikely explanation for certain of the nonlinear electrical properties of skeletal muscle, particularly the nonlinear transient properties called charge movement (Chandler et al., 1976 *a*; Adrian and Almers, 1976 *a* and *b*).

In this paper we examine in detail the hypothesis (mentioned in Franzini-Armstrong, 1971, p. 202, and in Huxley, 1971, p. 14) that a transient ionic current might couple T system and SR (Fig. 1). We show that this hypothesis, in suitable form, can survive the above criticisms. It is consistent with the electrical properties and action potential of skeletal muscle and can account for many aspects of excitation-contraction coupling. We are unaware, however, of convincing evidence that ionic current actually flows between T system and SR in skeletal muscle; new experiments are needed to settle this point.

BACKGROUND AND PROCEDURE

Electrical Properties

Our procedure is to construct a circuit model, compatible with the known morphology of a skeletal muscle fiber, which includes current flow from T system, across the T-SR junction into the SR (see Figs. 1 and 2). We adjust the parameters of the model to predict the measured electrical properties of skeletal muscle as well as possible, particularly the nonlinear "capacitive" properties recently reviewed by Almers (1978).

Two kinds of current flow occur across membranes: one is produced by the movement of ions across the membrane and therefore is called ionic or transmembrane current; the other is called capacitive or intramembrane current because it is produced by the accumulation and depletion of net charge on either side of the membrane, without the transfer of ions across the membrane. Capacitive current is most easily measured in preparations treated with blocking agents that remove transmembrane

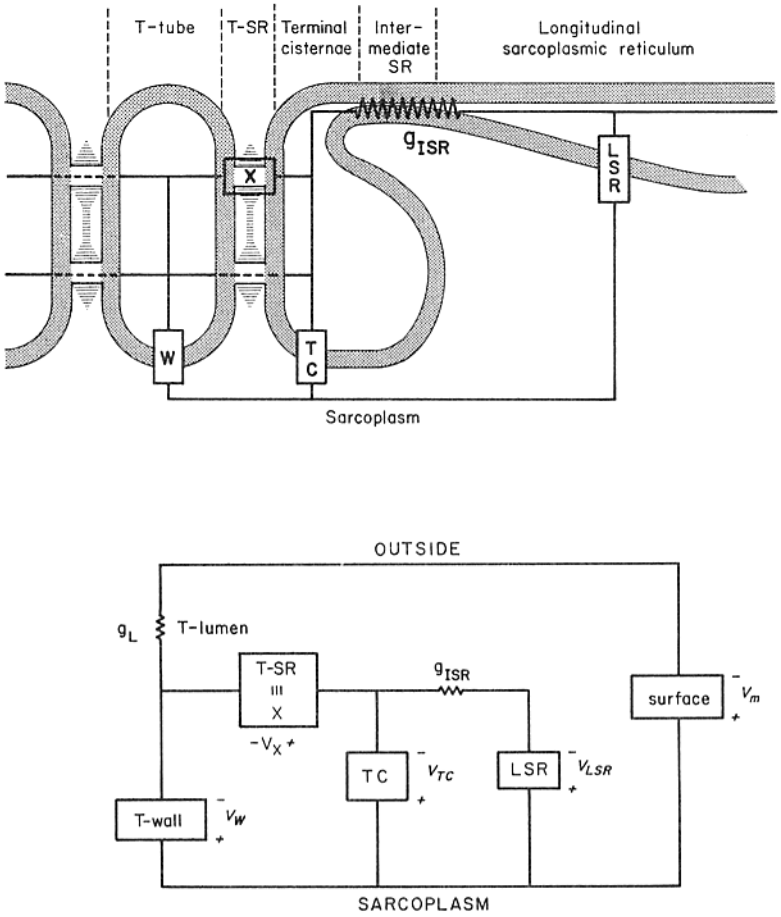

FIGURE 1. The circuit model. The upper panel shows a circuit model of the tubular system, terminal cisternae, and sarcoplasmic reticulum of skeletal muscle. The properties of specialized structures are indicated by boxes and are identified in more detail in Fig. 2 and in the text. Noteworthy features of the model are the presence of a conductive path g_x for ionic current flow from the lumen of the T system to the terminal cisternae and the presence of a substantial resistance $1/g_{ISR}$ isolating terminal cisternae from the longitudinal sarcoplasmic reticulum. The lower panel shows the circuit representation of a complete fiber, including the luminal conductance of the T system and the properties of the surface membrane. In our computations the T system is treated as a lumped circuit element; distributed properties are approximated by including g_L. This approximation will not be particularly accurate at very short times or during an action potential.

currents. Because capacitive current represents intramembrane charge movement (by definition), the capacitive charge that moves after a depolarizing step in potential must equal the capacitive charge that flows after repolarization to the resting potential. This property is not expected in ionic currents, and, therefore, the equality

of ON and OFF charge movements is one of the defining features of capacitive currents.

The capacitive current across single membranes has several components. One component would be present if the membrane were replaced with a vacuum. That component is called pure displacement current and can be described by a capacitance of ~0.1 $\mu F/cm^2$ in a membrane 8 nm thick. Pure displacement current flows at the speed of light; and it is strictly linear, showing no saturation. Other components of capacitive current are called polarization currents and are modulated by the movement of charges and molecules bound within the membrane. The ratio of the total capacitive current (polarization plus pure displacement) to the pure displacement current is the relative dielectric constant, ranging from a value near 2 for pure lipids to a value of 80 for water. Polarization currents are nonlinear and show saturation at large electric field strengths. The time-courses of such currents may be determined by

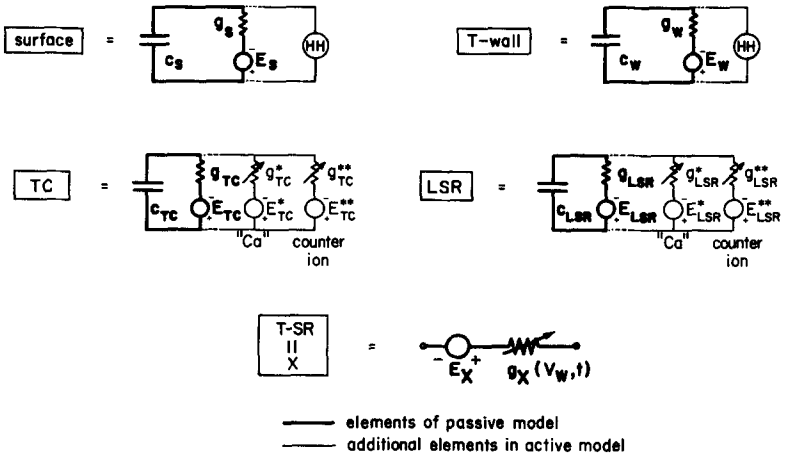

FIGURE 2. Description of the membranes of the circuit model. Each membrane is represented as a fixed (voltage-independent) capacitance in parallel with ionic pathways. In the passive model, the ionic pathway is a conductance in series with a battery. In the active model, a conductance for Ca^{++} and a counterion are included in the membranes of the terminal cisternae and longitudinal SR. The circle containing HH represents the Hodgkin and Huxley conductances for Na^+ and K^+, as modified by Adrian and Peachey (1973) for skeletal muscle. These HH conductances are used only in the computations of the action potential shown in Fig. 6.

the probability of a change of conformation in membrane macromolecules or by the speed of movement of charges trapped within the membrane.

The movement of a large charged group within the membrane has long been a candidate for the voltage sensor that controls the ionic conductances underlying the action potential (Hodgkin and Huxley, 1952). For that reason, Schneider and Chandler (1973), Armstrong and Bezanilla (1974), and Keynes and Rojas (1974) introduced an experimental paradigm to unveil the "gating" currents expected from movement of a voltage sensor. Such gating currents are nonlinear polarization currents defined by several properties. The integrals of such currents (i.e., the charge movement) will be equal during a depolarization and subsequent repolarization to the

initial potential. Such currents are expected to show substantial nonlinearity in the voltage range in which the ionic conductance is nonlinear, namely, a threefold change in conductance for about a 5-mV change in potential, which corresponds to a change in electric field of tens of thousands of volts per centimeter in a membrane 8 nm thick.

The paradigm introduced is a pulse schedule that removes displacement and linear polarization currents, thus unveiling gating currents previously hidden within the total transient current. The paradigm involves two measurements. The first measurement estimates the linear transient currents thought to be irrelevant to the gating process and is made at a potential at which the residual (unblocked) ionic current is expected to be resistive and linear, and at which the nonlinear component of polarization is expected to be absent. The second measurement is made in the range of voltages in which both linear and nonlinear polarization currents should be present. Subtraction of the two measurements, after scaling for any difference in size of applied voltage, gives estimates of the physiologically interesting nonlinear charge movement. If the residual ionic current is in fact linear, as was assumed, and if the ON charge movement equals the OFF charge movement, the subtracted records are used directly to measure gating or nonlinear polarization current. If the residual ionic current is nonlinear, measures are taken to separate the nonlinear polarization current from the nonlinear ionic current. If the ON charge movement does not equal the OFF, it has sometimes been shown (Armstrong and Benzanilla, 1977) that part of the charge movement has become immobilized or too slow to observe experimentally.

Computations

We compute the electrical properties of a circuit model (Mathias, 1979) that might represent a skeletal muscle fiber. The circuits are solved by analytical techniques when appropriate (see the Appendix). Straightforward numerical methods are used in other cases. Starting from the initial conditions, we compute the potentials and currents at later times by simple iteration of steps in time Δt, replacing derivatives by first order forward differences. The step size Δt was decreased until results were insensitive to further reduction.

Nonlinear conductances of the surface and T-system membranes are described by the kinetic schemes introduced by Hodgkin and Huxley (1952) as used for skeletal muscle by Adrian and Peachey (1973). The conductances and equilibrium potentials are indicated by the abbreviation HH in Fig. 2. The nonlinear conductances of the T-SR junction and SR membranes are computed using simpler analytical descriptions, which seemed better suited for selection of optimal parameters than the Hodgkin-Huxley formulation. Fig. 3 illustrates many of the properties of the hypothetical channel g_x at the T-SR junction, using variables described in Eqs. 2–8.

The nonlinear time-dependent ionic current through the T-SR junction is described by a scaling conductance $\bar{g}_x$; a rectification factor $\xi_x(V_x)$ describing the nonlinearity of the instantaneous current voltage relation; a probability density function $p_x(V_w, t)$ for the conducting state; and a probability density function $p_{1x}(V_w, t)$ for an intermediate nonconducting state. The probability density functions are determined by $a_x(V_w)$, the probability, per unit time, of a change in state, and $N_x(V_w)$, the fraction of the total number of channels able to open at voltage V_w.[1]

[1] Variables of the same form were used to describe the nonlinear conductances of the SR membranes in the active and passive models (Figs. 2 and 5 *C*).

The current is then

$$i_x(t, V_w, V_x) = \{\bar{g}_x \xi_x(V_x) p_x(t, V_w) + g_{xo}\}\{V_x - E_x\}\Delta g_x(t, V)\{V_x - E_x\}, \quad (1)$$

where E_x is the equilibrium potential of the pathway. Note that the conductance g_x is controlled by the potential in the T system. In other computations, not illustrated in this paper, g_x was controlled by the potential across the T-SR junction. Because there were no significant differences in the results of the calculations, only the former

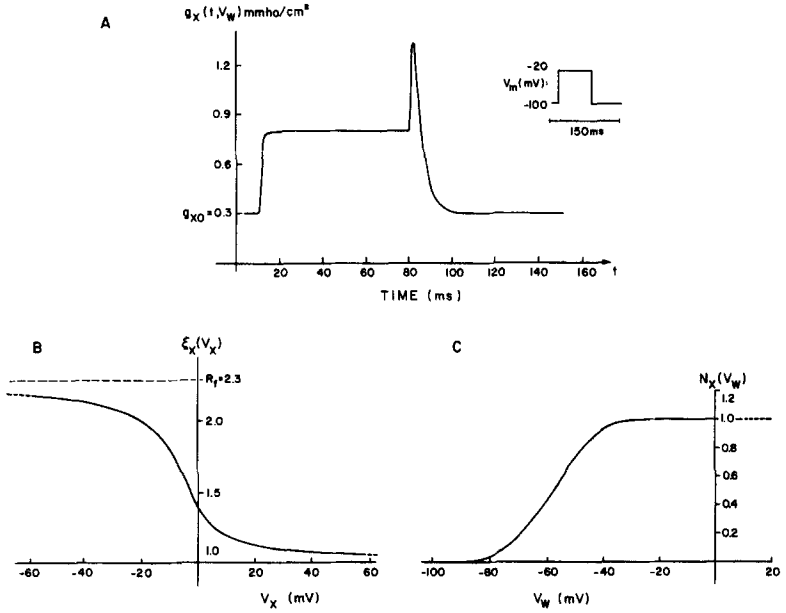

FIGURE 3. The time and voltage dependence of the ionic pathway postulated from T system to SR. *A* shows the time-course of the conductance g_x for the step of potential (of 70 ms duration and height ΔV) illustrated symbolically. Note the rapid increase in the conductance and the rather slower decline (more evident in Fig. A 2). A jump in the conductance occurs when the pulse is turned off because of instantaneous rectification, which depends, in effect, on the direction of current flow. *B* and *C* illustrate the functions that describe the instantaneous and time-dependent rectification of g_x, respectively, as described in Eqs. 1–8.

are presented here. The probability density functions are defined by

$$\frac{dp_x}{dt} = -a_x(V_w)(p_x - p_{1x}) \quad (2)$$

$$\frac{dp_{1x}}{dt} = -a_x(V_w)\{p_{1x} - N_x(V_w)\}. \quad (3)$$

The probability of a change in state ranges from a_{min} to a_{max} and has voltage dependence determined by the constant K_a.

$$a_x(V_w) = a_{min} + \frac{a_{max} - a_{min}}{1 + \exp\{(\bar{V}_a - V_w)/K_a\}} \quad (4)$$

The voltage dependence of the number of open channels is described by

$$N_x(V_w) = \left[\frac{1}{1 + \exp\{(\bar{V}_N - V_w)/K_N\}}\right]^2. \quad (5)$$

Note that $p_x(\infty, V_w) = N_x(V_w)$ or, in other words,

$$g_x(\infty, V_w) \rightarrow \bar{g}_x N_x(V_w), \quad \text{as} \quad t \rightarrow \infty \quad \text{if} \quad \xi_x = 1. \quad (6)$$

The instantaneous rectification is determined by

$$\xi_x(V) = \frac{R_f + 1}{2}\left\{1 + \frac{1}{\phi} - \frac{1}{\phi}\sqrt{1 + \left(\frac{R_f - 1}{R_f + 1}\right)^2 (\phi^2 + 2\phi)}\right\}. \quad (7)$$

This hyperbolic definition of rectification depends on the absolute value of potentials, and, therefore, the expression (Eq. 7) should be evaluated in the form presented. The

TABLE I

LINEAR OR RESTING MUSCLE PARAMETERS

	Capacitance	Conductance	Equilibrium potential
	$\mu F/cm^2$	$\mu mho/cm^2$	mV
Fiber	$c_{eff} = 7$	$g_{eff} = 330$	$E_{rest} = -90$
Surface membrane	$c_s = 1$	$g_s = 140$	$E_s = -90$
Isolation	---	$g_L = 650$	---
T-system membrane	$c_w = 4.5$	$g_w = 30$	$E_w = -90$
Isolation	---	$g_{xo} = 300$	$E_x = -90$
Membranes of terminal cisternae	$c_{TC} = 8$	$g_{TC} = 250$	$E_{TC} = 0$
Isolation	---	$g_{ISR} = 100$	---
Membranes of longitudinal SR	$c_{LSR} = 30$	$g_{LSR} = 700$	$E_{LSR} = 0$

Values are computed for the area of structure associated with 1 cm^2 of outer surface, assuming the muscle fiber is a right circular cylinder of radius $a = 40$ μm.

rectification factor R_f is

$$R_f = \frac{g_x(V, \infty)_{max}}{g_x(V, \infty)_{min}}. \quad (8)$$

The normalized potential is $\phi = (V - \bar{V})/\kappa$, where κ sets the potential range, in mV, over which ξ_x changes from 1 to R_f. $\bar{V}$ is the potential, in mV, about which the rectification is centered.

The parameters of the model shown in Tables I and II seem to optimize the fit between theory and experiment, the optimization being done by hand. The morphometric parameters of the model were constrained to the values measured by Mobley and Eisenberg (1975). Constraints were placed on the electrical parameters: the specific capacitance of membranes was required to be close to 1 $\mu F/cm^2$; the specific conductance of membranes was less constrained but was kept between 7 and 300 $\mu mho/cm^2$. A suitable optimization program might conceivably reveal quite different sets of parameters compatible with experiment.

RESULTS

The results of our calculations are a set of curves to be compared directly with experimental data of Schneider and Chandler (1973), Chandler et al., (1976

a), and Adrian and Almers (1976 *a* and *b*). We choose to fit electrical data because it has been taken as the main evidence against ionic current flow from T system to SR. Such data depend primarily on the early stages of excitation-contraction (EC) coupling, but are physically, mechanistically, and temporally distant from the later stages. It is not surprising that our analysis becomes progressively more difficult, arbitrary, and perhaps unconvincing as we move from the T system to the terminal cisternae and then into the longitudinal SR.

The choice of experimental data is somewhat arbitrary since so much descriptive information is available concerning EC coupling. Much of that data is indirect, however, involving measurements of tension that are the outcome of unknown mechanisms in the filaments and cross-bridges as well as

TABLE II
NONLINEAR PARAMETERS

	Instantaneous Recitification Terminal cisternae	T-SR junction
	ξ_{TC} (V_{TC})	ξ_x (V_x)
R_f, *unitless*	2.5	2.3
$\bar{V}$, *mV*	70	0
κ, *mV*	−2	3
	Time-dependent Recitification	
	N_x (V_w)	a_x (V_w)
Rate constants, s^{-1}	---	a_{min}= 350
	---	a_{max}= 2,2200
$\bar{V}$, *mV*	−65	−55
κ, *mV*	8	9.5

The scaling parameter $\bar{g}_x$ = 500 μmho/cm^2.
Values are computed for the area of structure associated with 1 cm^2 of outer surface, assuming the muscle fiber is a right circular cylinder of radius a = 40 μm.

EC coupling. Indirect data cannot be used to analyze EC coupling unless the contribution of contractile processes is known.

We have also chosen to ignore some electrical phenomena, namely, multiple components of charge movement and the slow phenomena, called inactivation, reactivation, and/or repriming, because they almost certainly involve multiple processes known too vaguely to model (Chandler et al., 1976 *b*; Adrian et al., 1976; Adrian and Rakowski, 1978; Rakowski, 1978; Adrian and Peres, 1977 and 1979; Adrian, 1978).

The phenomena we seek to explain are:

(*a*) The linear electrical properties of a muscle fiber, in particular the effective capacitance of ~7 μF and an effective resistance of ~3 kohm for each cm^2 of outer surface in a fiber of 40 μm radius at a sarcomere length of 2.5 μm (Valdiosera et al., 1974; Hodgkin and Nakajima, 1972 *a* and *b*; Schneider and Chandler, 1976; Chandler and Schneider, 1976).

(*b*) The control of calcium release by the potential across the T-system membrane. Calcium release can be turned on and turned off by changes in T-

system potential under a variety of experimental conditions (Costantin, 1975; Endo, 1977; Caputo, 1978).

(*c*) The change in SR potential when a potential is applied across the surface membrane. If calcium release is to be produced by a voltage-dependent change in the properties of the SR membrane, as in the models considered here, there must be a reasonable change in SR voltage when the T system is depolarized.

(*d*) The time-course, amount, and voltage dependence of the nonlinear transient currents described as charge movement. These should have a natural role in the model, we hope as a direct part of EC coupling.

(*e*) The time-course, amplitude, and rate of rise of the muscle action potential.

Models

We have considered many forms of the circuit model shown in Figs. 1 and 2. The Appendix (Fig. A 1) presents the simplest situation, in which g_x is the only time- or voltage-dependent conductance in the circuit: all membranes are treated as linear constant elements. Chandler et al. (1976 *a*, Figs. 16 and 17) have considered similar simple models but with different properties of g_x. The properties of g_x assumed in that paper did not produce equality of the nonlinear charge movement at the ON and OFF of a depolarizing pulse.

We suppose that the conductance linking T system and SR increases rapidly soon after a depolarization and decreases slowly after a subsequent repolarization (Fig. A 2). The circuit shown in Fig. A 1, with the properties of g_x shown in Fig. A 2, we call the "linear" model. When compared with experimental data, the linear model differs in two ways. (*a*) If charge is plotted as a function of voltage, the curve is found to bend but not saturate at large depolarizations (Fig. A 3). (*b*) The assumed properties of g_{TC} and g_x imply (through Eqs. A 2 and A 3) that the time-course of the ON and OFF transient currents are similar; the OFF charge movement is not faster than the ON. (In the linear model the conductance g_{TC} is constant, and the conductance g_x is supposed to remain large for a long time after repolarization (see Fig. A 2). Thus, the time-course of the OFF transient is determined in large measure by the same parameter values that determine the time-course of the ON transient.)

The linear model does not include processes quite likely to be present in the real SR. In particular, it is likely (Endo, 1977; Stephenson, 1978) that the SR includes a voltage-dependent calcium conductance. An "active" model was therefore constructed, which includes time- and voltage-dependent conductances as shown in Fig. 2. This model was analyzed in some detail and conclusions from that analysis are described in the Discussion. The properties of the "passive" model, described below, could be made similar to those of the active model. For that reason, the calculations on the more complex and arbitrary active model are not presented here. The passive model, defined by the heavy lines in Fig. 2, includes instantaneous rectification in g_x and g_{TC} (see Figs. 3 and 5 *C*), which produces, respectively, (*a*) a faster time-course of the OFF transient than the ON transient and (*b*) saturation in the curves relating charge to voltage.

Elements of the Passive Model.

Fig. 3 shows the voltage and time dependence that we have assigned to g_x in the passive model to compute the nonlinear charge movement shown in Fig. 4. The abrupt increase in $g_x(t, V_W)$ after repolarization (Fig. 3 *A*) is a consequence of the instantaneous rectification function $\xi_x(V_x)$ shown in Fig. 3 *B*. The instantaneous rectification in g_x allows inward current to flow more easily than outward. Because g_x is much more conductive during the OFF phase of charge movement, the time constant for the OFF transient current is faster than that for the ON, as predicted semiquantitatively by Eq. A 3. However, if g_x is more conductive during the OFF phase of charge movement, Eq. A 4 or A 7 predicts an increase in Q_{off} without an increase in Q_{on}. Such an increase is not found experimentally. To reconcile theory with experiment, we adjust the rate constant for the turn off of g_x. We use a value of a_{min} (Table II and Eq. 4) faster than that used in the Appendix (cf. Figs. 3 *A* and A 2). In this manner, some of the charge movement that would otherwise flow through g_x is cut off. Thus, the time-course of Q_{off} depends, in part, on the speed with which g_x turns off. This procedure may seem quite arbitrary and delicate, requiring an artificial and unlikely balance between a_{min} and ξ_x, but such is not the case. The ratio of ON to OFF charge movement is near unity for a wide variation in either parameter. In this regard, one should also be aware that the experimental values of Q_{on}/Q_{off} often differ noticeably from unity.

In Fig. 3 *C* we show the sensitivity function $N_x(V_w)$ for the fraction of channels that eventually would become conductive at a given T-system potential. Note that the change from the resting to the more conductive state is a function of the T-system potential V_w, while the instantaneous rectification depends on V_x. We made the second choice on the presumption that the instantaneous rectification would be a function of current flow through the channel; the first choice is arbitrary because we do not know which voltage is sensed by, and thereby controls, the time-dependent component of the conductance g_x.

Nonlinear Transients in the Passive Model

Fig. 4 is a compilation of our results, comparable and similar to the experimental data we have tried to describe. Table I presents the linear parameters used in these computations. The specific capacitance of the membrane of the T system and longitudinal SR was taken to be 1.0 $\mu F/cm^2$, and the specific capacitance of the membrane of the terminal cisternae was 0.74 $\mu F/cm^2$, using the estimates of membrane areas given by Mobley and B. Eisenberg (1975). Computations using a specific capacitance of 0.9 $\mu F/cm^2$ for all membranes can give almost the same results.

The resting effective resistance of this theoretical fiber (radius, 40 μm) was about 3 kohm-cm^2, referred to the outer surface of the fiber (see Table I and Eq. A 3). The resting effective input capacitance is ~ 7 $\mu F/cm^2$ of outer surface (see Table I and Eq. A 6). Fig. 4 *A* is the time-course of charge movement for steps of membrane potential from a holding potential of -100 mV. Fig. 4 *B*, *C*, and *D* summarize several properties of the charge movements shown in Fig. 4 *A*.

Fig. 4 *B* shows the dependence of computed charge movement on the potential across the surface membrane. We see that the passive model can produce nonlinear charge movement that saturates. The saturation of charge movement is predicted in a semiquantitative manner by Eq. A 7, which shows

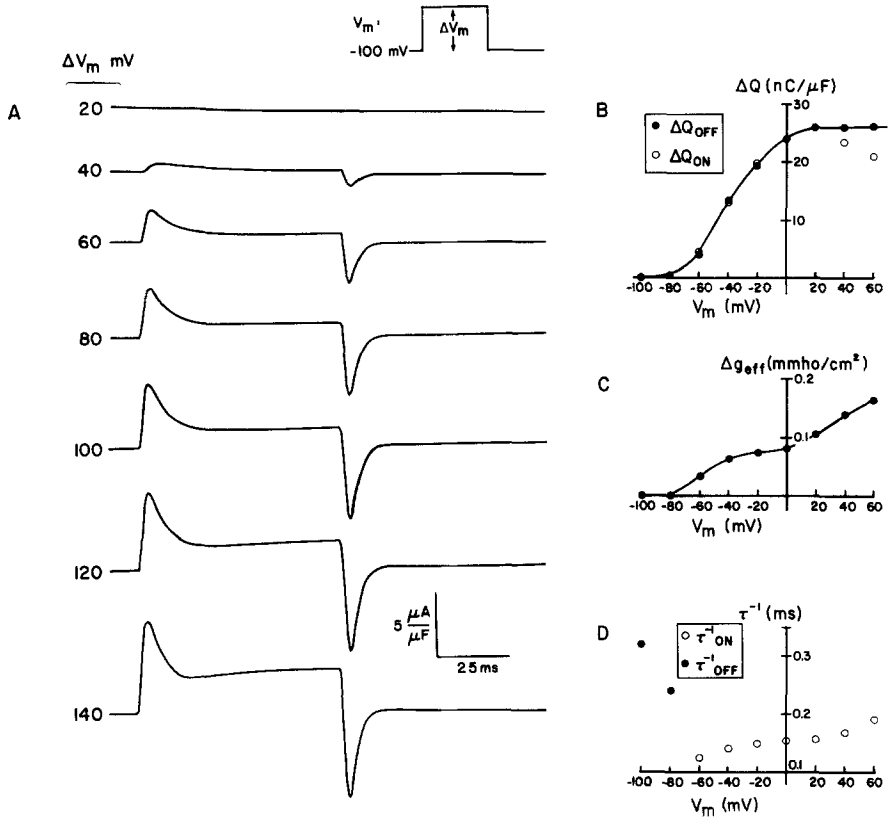

FIGURE 4. The predicted nonlinear transient currents. These records are to be directly compared with the experimental results of Chandler *et al.*, 1976 *a*, and Adrian and Almers, 1976 *a* and *b*. The currents shown in *A* are the sum of the currents produced by the pulse shown (of 70 ms duration and height ΔV) and a pulse of the same size in the hyperpolarizing region. Because the circuit elements are assumed to be independent of voltage in the hyperpolarizing region, the summation emphasizes the nonlinear components of current. *B* illustrates the integrals of the transients shown in *A*, computed after subtraction of a constant baseline. The area represented by this procedure is illustrated in Fig. A 2. Note the rough equality of ON and OFF charge and the saturation of charge movement. Because of the slope of the baseline at depolarizations to +20 mV and +40 mV, we underestimate the values of ΔQ_{on}. The solid line is therefore drawn through the filled circles representing ΔQ_{off}. *C* shows the amount of nonlinear ionic current (graphically identified in Fig. A 2) accompanying the nonlinear transient current. Note the increase in nonlinear ionic current that accompanies the saturation of nonlinear charge movement. *D* illustrates the estimated time constants of the nonlinear transient currents.

that an increase in g_{TC} (Fig. 5 *C*) causes a decrease in c_{eff} (if g_x is constant) and, thereby, produces saturation in charge movement. The increase in g_{TC} is reflected in the sloping baseline seen in the response to step changes of 120 mV and 140 mV (Fig. 4 *A*). The increase in g_{TC} also introduces errors in our computation of Q_{on} (because a constant baseline was subtracted before integration). Therefore, we have drawn the solid line in Fig. 4 *B* through the points representing Q_{off}, which is a more accurate estimate of the charge movement.

The change in input conductance necessary to produce the charge movement Fig. 4 *A* and *B* is shown in Fig. 4 *C*. The increment in g_{eff} between $V_m = -100$ mV and $V_m = -20$ mV is almost entirely caused by the increase in g_x. The increment in g_{eff} at potentials (across the surface membrane) more positive than −20 mv is caused by the rectification in g_{TC}. In this voltage range, g_x is fully activated (i.e., $N_x[V_w]$ has reached its maximum value of one), and g_{TC} begins to increase as a function of V_{TC}. As previously mentioned, the increase in g_{TC} is reflected in the charge movement transients (Fig. 4 *A*) as a change in the slope of baseline current (the current labeled Δi_{leak} in Fig. A 2). The slope of the baseline current is associated with saturation of charge movement and both should occur in the same voltage range (in our passive model computed with the parameters presented in Tables I and II). The situation for more general values of the parameters is discussed in the Appendix, after Eq. A 9.

Experiments on skeletal muscle show a slope in baseline current that has been attributed to the residual potassium conductance not removed (at positive potentials) by the blocking agent applied (usually tetraethylammonium ion). In our computations, the nonlinear leakage current, or change in conductance Δg_{eff}, is less than that found experimentally by Chandler et al. (1976 *a*, Fig. 6) and by Adrian and Almers (1976 *b*, Figs. 2, 3, and 8). In our scheme—the passive model with parameters used here—some fraction of the experimentally observed leakage current would be ascribed to residual ionic current across the tubular or surface membranes and some to current flow into the SR.

Kinetics of ON and OFF Transients in the Passive and Active Models

The rate constants of the charge movement are shown in Fig. 4 *D*. These have been estimated by plotting the charge movements on semilogarithmic paper and are subject to the same substantial errors as experimental measurements of rate constants, and for the same reasons: the movement of charge during the depolarization is not well described by a single exponential, and the procedure for fitting a single exponential to such records is necessarily arbitrary. The ON rate constants (○) are computed from the response to steps of potential from a holding potential of −100 mV. The OFF rate constants (●) were computed for a step of potential from −80 mV to a positive potential and back to −80 mV (with the appropriate subtraction of the response in the hyperpolarized range of potentials) and for a step from −100 mV to a positive potential and back to −100 mV. The OFF rate contants were insensitive to the positive potential chosen.

The voltage and time dependence of the experimental ON transient fits naturally with the passive model: the kinetics of the ON transient are a necessary consequence of those features of the passive model introduced to give equality of ON and OFF charge and a saturating dependence of charge movement on voltage (Fig. 4 *B*). For small depolarizations, the increase in g_x (which is a property of all the models considered here; see Figs. 3 *C* and A 2) produces an increase in rate constant as described by Eqs. A 2 and A 3. For larger depolarizations, the increase in g_{TC} (introduced into the passive model to produce saturation of charge movement at large depolarizations; see Fig. 5 *C*) becomes significant and produces a progressive increase in the ON rate constant, even in the voltage range in which charge movement has saturated.

The experimental OFF transient is harder to fit. The linear model, presented in the Appendix (Fig. A 3), seriously misfits the OFF kinetics. The rather complex properties of g_x in the passive model (Fig. 3) allow a reasonable fit, but the reality of such unprecedented and complex properties may be doubted.

The active model introduces voltage- and time-dependent properties into the conductance g_{TC} to achieve a good fit of the OFF response. In the active model, which is not presented in detail here, the conductance for counterions (labeled g_{TC}** in Fig. 2) was made to turn off more slowly with repolarization than the calcium conductance g_{TC}*. Thus, upon repolarization, the negative equilibrium potential E_{TC}* pulled V_{TC} back to its resting value quite rapidly. In this way, the active model could fit the experimentally determined kinetics of the OFF response without introducing instantaneous rectification into the properties of g_x.

Computations of Potential Changes

Fig. 5 illustrates the potential changes in the T system, terminal cisternae, and longitudinal SR computed from the passive model. The dependence of the potential of the terminal cisternae on depolarization is shown, as is the rectification postulated in the membrane of the terminal cisternae.

An action potential can be calculated using the model just presented. Fig. 6 shows, at two different time scales, the action potential calculated for a preparation in which there is no propagation. The dashed curve shown at the faster time scale is the action potential across the T-system membrane. It is apparent that the current flowing from T system to SR does not slow the rising phase or load the action potential. Indeed, the shape of the action potential is actually made more realistic by the inclusion of such currents.

The computations shown in Fig. 6 were made using Hodgkin-Huxley parameters at 3°C (Adrian and Peachey, 1973). Therefore, the surface action potential is slow and almost coincides with the T-system waveform. The expected change in potential within the terminal cisternae of the SR is also shown. A simple lumped model has been used to represent the T system in these calculations because the purpose of the calculation is to show the effects of current flow into the SR. The shape of the action potential computed including current flow into the SR is nearer to that experimentally recorded (Adrian et al., 1970 *a* and *b*) than the shape computed without such current.

However, any computation incorporating charge movement would produce much the same action potential. We imagine that calculations of propagating action potentials that include charge movement and increased amounts of g_{Na} in the tubules will give action potentials of realistic shape and conduction velocity, without invoking an access resistance at the mouth of the tubules.

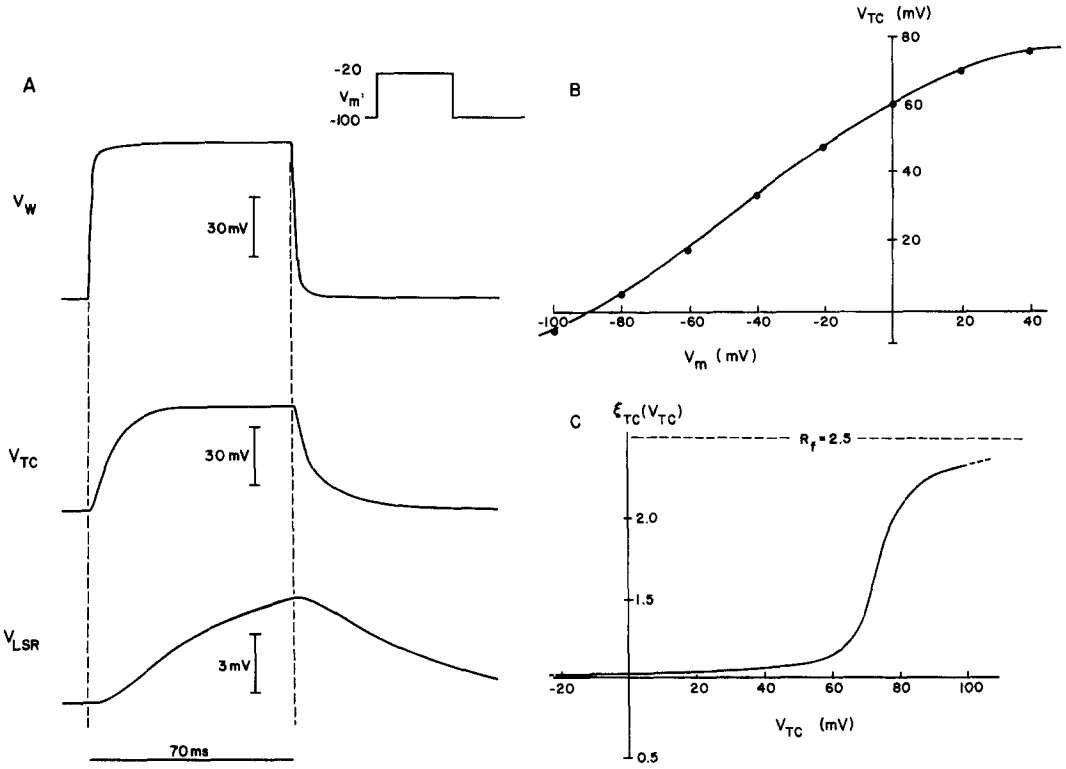

FIGURE 5. The predicted voltages. *A* illustrates the voltages computed across the wall of the tubules (V_w), across the membranes of the terminal cisternae (V_{TC}), and across the membranes of the longitudinal SR (V_{LSR}) for the 70-ms pulse of voltage V_m illustrated across the surface membrane. *B* illustrates the variation of the steady-state value of V_{TC} with V_m. *C* illustrates the rectification assumed in the terminal cisternae for the calculations of the passive model. The symbols are identified and used in Eqs. 1–8.

DISCUSSION

Other Phenomena

EC coupling includes many phenomena not discussed here. A correct model should account for all of these. Some can, in fact, be interpreted or explained easily by our model. Other phenomena, such as slow currents, immobilization of charge, and so on, require additional specific properties of g_x, the conductance linking the T system and the SR.

There are many electrical phenomena that might reflect current flows or changes in ionic concentrations in SR compartments. Slow ionic currents (Adrian et al., 1970 *a* and *b*), components of charge movement (Adrian, 1978), calcium currents (Sanchez and Stefani, 1978; Palade and Almers, 1978), and slow phenomena of charge movement (Chandler, et al., 1976 *b*; Adrian et al., 1976; Adrian and Rakowski, 1978; Rakowski, 1978) might all have counterparts in current flows or concentration changes in the SR. The interpretation of such currents would be complicated by their flow through at least two serial systems—the T-SR junction and the SR membranes—of presumably different properties. Similar complications would appear in the interpretation of faster currents if they flowed into the SR. For example, if some of the current usually

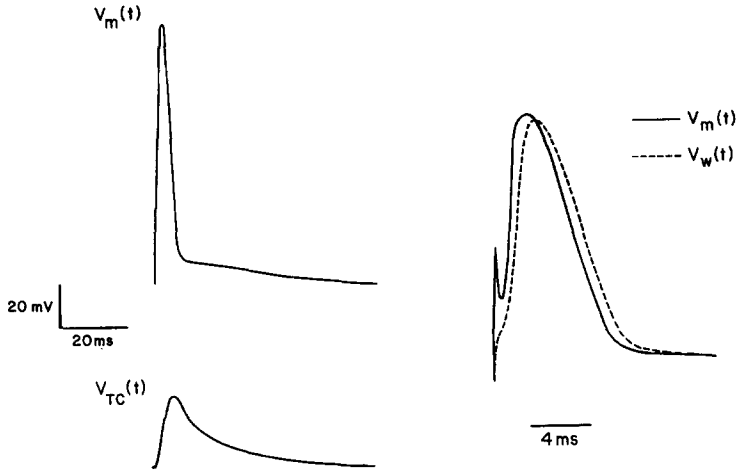

FIGURE 6. Computed action potentials. The waveforms shown illustrate the computed nonpropagating action potential as seen across the surface membrane (V_m), across the wall of the tubular system (V_w), and across the membranes of the terminal cisternae. The calculations are done with the values of the Hodgkin-Huxley parameters used by Adrian and Peachey (1973) at a temperature of 3°C. The action potentials on the right are shown on a fast time scale to illustrate the T system and surface voltages.

identified as "K^+ currents through the delayed rectifier" flowed into the SR (Freygang, 1965), total K^+ current and EC coupling would have a real but confusing relationship (Adrian, 1964; Adrian et al., 1969; Kao and Stanfield, 1968 and 1970).

The optical signals thought to reflect the membrane potential of the SR (Benzanilla and Horowicz, 1975; Baylor and Oetliker, 1977; Vergara et al., 1978; Baylor et al., 1979) should correspond to the weighted average of potentials across the membranes within the model. The weights would depend on the areas (Mobley and B. Eisenberg, 1975) and optical properties of each membrane of the SR.

The detailed phenomenology of EC coupling (reviewed in Costantin, 1975; Caputo, 1978; Lüttgau and Moisescu, 1978), including the properties of K^+

contractures and the relation of charge movement and contraction (Kovacs et al., 1979), should be explicable. Note that the usual identification of K^+ contractures and depolarization-induced contractures would need reexamination if K^+ were the main carrier of current from T system to SR.

Structural observations (Somlyo, 1979; B. Eisenberg et al., 1979), including experiments showing the apparent formation of pillars at the T-SR junction upon depolarization (B. Eisenberg and Gilai, 1979; B. Eisenberg et al., 1979), should give results congruent with the properties of the conductance g_x. (At least, that is so if one adopts the additional hypothesis that changes in g_x correspond to the formation or breakage of pillars.)

Linear Model

The linear model, described in the Appendix, seems minimally complicated. It allows only one circuit element g_x to vary with potential and time; not surprisingly, it does not describe all the experimental data. Nonetheless, the analytical constraints derived for the linear model are applicable, in large measure, to more complicated models. If current flow into the SR is in fact the correct explanation of charge movement in muscle, the eventual description of that current is likely to be more complicated than the models we present. It seems to us, however, that the linear model will always be useful in deriving analytical approximations and providing intuitive insights, if EC coupling does indeed include significant current flow into the SR.

Passive Model

The inadequacies of the linear model can be removed with a few changes, which define the passive model. The passive model includes instantaneous rectification in g_x and the SR membranes (see Results) and fits experimental results. The saturation and asymmetry in the time-courses of charge movement are caused by the rectification in g_{TC} and g_x, respectively. Because potential changes in the SR are quite slow compared with an action potential, it would not be easy to distinguish an instantaneous rectifier in the SR membrane from a typical potassium conductance. The particular current voltage characteristic used here to describe the instantaneous rectifier is certainly not unique—indeed, it may not even be the optimal location to introduce the rectification.

For example, the rate constants computed and illustrated in Fig. 4 *D* do not quite match those reported by Chandler et al. (1976 *a*, Fig. 13) and by Almers and Best (1976, Fig. 3). If the charge movement at membrane potentials between −60 mV and −40 mV were produced by a decrease in g_{TC} rather than an increase in g_x, then the rate constants would be slower at −40 mV than at −60 mV, as was measured.

Active Model

The active model (Results and Figs. 1 and 2) introduces and examines the consequences of an SR calcium current. We assume a voltage- and time-dependent calcium selective channel, with conductance described by equations of the form of Eqs. 1–7, letting $\xi \equiv 1$. The calcium current is presumed to be driven by the calcium equilibrium potential. Difficulties arise if the

calcium conductance is the only "active" conductance. Once such a calcium current is turned on, the potential across the SR membrane tends to be clamped at the calcium equilibrium potential, which removes the driving force for calcium movement and makes the SR membrane potential rather independent of the T-system potential. Therefore, we include a conductance for a counterion, also described by Eqs. 1–7, with $\xi \equiv 1$. This ion is assumed to have an equilibrium potential in the opposite direction from that for calcium; thus, the potential across the SR membranes is kept away from the calcium equilibrium potential. The SR potential is thereby kept under the control of the T-system potential, even when substantial active calcium currents flow across the SR membranes.

The computations of the active model were in large measure successful. They replicated the experimental curves of charge movement, including a more rapid time-course for the OFF transient current and saturation of charge movement at large depolarizations. (Note that the active model could reproduce these properties without the instantaneous rectification used in the passive model, i.e., with $\xi_x \equiv 1$.) The constraints implicit in Eq. A 5 (with the measured values of g_{eff}, c_{eff}, and τ) are more important to the linear and passive models than to the active model. We relaxed the constraints considerably in our calculations with the active model, hoping to produce enough active calcium current to charge the membranes of both the terminal cisternae and the longitudinal SR, without needing a small value of the conductance g_{ISR}. The active model did allow the charging of a larger amount of SR capacitance in a shorter time period than simpler models, but the computation of realistic charge movement still required a small value of g_{ISR}.

The computations of the active model were unsuccessful in an important respect. The calcium currents that we computed were too small, by a factor of ~100, to account for the 100-μM release of calcium in a twitch (Costantin, 1975; Endo, 1977; Luttgau and Moisescu, 1978). When the calcium conductance was increased enough to produce such fluxes, the counterion conductance had to be adjusted so that the calcium current and counterion current were almost equal (±1 % deviation in magnitude) at all potentials and times. We could not achieve this balance with independent conductances. If the current generated by the release of calcium were balanced charge for charge by an exactly equal and opposite current of another ion, then there would be no electrical effect of calcium release. Calcium release produced by this kind of "electrically silent" process would be easy to include in our model. It would not disturb our predicted currents because it would not produce current flow. It could still be controlled by a voltage sensing macromolecule (in the SR membrane) and, so, could have the necessary voltage dependence.

If the current generated by the release of calcium were mostly, but not entirely, balanced by the flow of another ion, then there would be a residual current associated with calcium release. The residue of unbalanced current in this type of electrically silent process would be sensitive to and produce potential changes within the SR. It would contribute significantly to the computed nonlinear charge movement but would not disturb the agreement with experimental data, if it carried < 1 % of the total flux of calcium.

We conclude that calcium release in the active and passive models must be electrically silent if excitation spreads to the SR by ionic current flow through the T-SR junction (see the mechanism proposed for cardiac muscle by Morad and Goldman, 1973).

Other Models

This paper considers models of electrical coupling between T system and SR in which the coupling conductance has a time-course and voltage dependence of the general type illustrated in Fig. A 2. We consider such models because they easily satisfy one of the defining characteristics of charge movement, namely, the equality of charge movement at the ON and OFF of a depolarizing pulse. Other models of electrical coupling have not been investigated in detail, although they have been considered in a qualitative way. For example, there might be satisfactory models in which g_x has rather simple properties and the current through g_{TC} has an N-shaped voltage dependence and complex kinetics.

Evaluation of Models

There are a number of features of the models we have considered that are quite specific and perhaps implausible. For example, we have assumed that all of charge movement is a consequence of ionic current flow from T system to SR. It seems more likely that a component of charge movement is produced by membrane-bound charge (for example, that involved in controlling g_{Na} or g_x) and another component produced by charging the capacitance of the terminal cisternae. Our assumptions have been made to show that electrical coupling between T system and SR is possible. We are fully aware that our model and assumptions require experimental check. Indeed, these models may well contribute to our knowledge of the mechanism of EC coupling only by exclusion.

The value of g_x used in all of our calculations represents quite a small coupling between T system and SR. The maximum coupling conductance is $<10^{-3}$ mhos/cm^2, which gives a conductance of 10^{-14}–10^{-15} mhos per pillar, assuming that all the T–SR sites described by Franzini-Armstrong (1970) contain conducting pillars. This figure is much less than the figure usually quoted for the conductance associated with a single-gap junction particle, but of course depends on the several levels of assumptions. If, for example, only a few of the T–SR sites contained conducting pillars (B. Eisenberg, et al., 1979), the conductance per pillar would be much higher. Our model is consistent with the view that the T–SR junction is a specialized junction, with structure and properties distinct from gap junctions (e.g., Peachey, 1968).

The passive and active models both separate the SR into two compartments, electrically isolated by a small conductance g_{ISR}. The value of this conductance, when it refers to one sarcomere of one myofibril, implies that the membranes of the intermediate region of the SR are nearly touching.

There is much evidence that terminal cisternae and longitudinal SR of frog twitch muscle are separated by a diffusion barrier:

(*a*) Winegrad (1968), using autoradiographic techniques, found that calcium

movements from longitudinal tubules to terminal cisternae can take more than 20 s after a tetanus, suggesting a diffusion barrier between those structures.

(*b*) Kirby et al. (1975), using tracer experiments on single muscle fibers and small muscles, conclude that calcium washes out of the terminal cisternae with a time constant of 2.7 min, whereas it washes out of the longitudinal SR with a time constant of 1,244 min. Winegrad (1970) also found that calcium in the terminal cisternae exchanges with the external medium much more quickly than calcium in the SR. The quantitative agreement between Winegrad (1970) and Kirby et al. (1975) is important because their techniques are subject to different artifacts: autoradiography determines the anatomical site of the compartments rather convincingly, whereas flux measurements convincingly determine the time constants of wash out. Calcium binding within the longitudinal tubules is another explanation of these results.

(*c*) Costantin et al. (1965) observed that precipitate of calcium oxalate is found in only the terminal cisternae and concluded that the cisternae are "differentiated regions" of the sarcoplasmic reticulum.

(*d*) The ultrastructure of the intermediate region of the SR suggests a diffusion barrier to some authors (e.g., Peachey, 1965 *a*, using conventionally fixed material; Howell, 1974, using ruthenium-treated material; and Sommer et al., 1978, using frozen material); but images of the intermediate cisternae in frog muscle are sufficiently variable that it is difficult to be sure which describes the living state.

(*e*) The findings of Huxley and Taylor (1958), showing much more extensive radial than longitudinal spread of local contractions, are also consistent with a constriction between terminal cisternae and longitudinal tubules.

No constriction is seen in certain other preparations (in, e.g., the black mollie *Mollienesia sp.* [Franzini-Armstrong and Porter, 1964; Peachey, 1965 *b*]). Unfortunately, charge movement has not been measured in preparations without constrictions. In this regard, it should be remembered that the low value of g_{ISR} in our model is needed only to reconcile the measured time-course and quantity of charge movement with the morphology of frog muscle. The low value is not needed to produce a substantial voltage change in the SR.

We have not specified the current carrier through the conductance g_x in our model. The requirement is simply made that no current flows at rest: the sum of the resting potentials across the T–SR junction and across the SR membrane must be zero. This requirement would be satisfied if K^+ were the principal carrier of current. The idea that a component of potassium current is related to EC coupling has a certain appeal in view of the similarity, mentioned before, between some properties of potassium current, some properties of EC coupling, and some properties of charge movement (see also Adrian and Peres, 1977; Adrian, 1978; and Adrian and Peres; 1979). By no means, however, is K^+ the only possible current carrier through the conductance g_x. Both Cl^- and Ca^{++} might well have equilibrium potentials of the right polarity to be the principal current carrier (Somlyo et al., 1977). In fact,

g_x might be a rather nonselective conductance in which most any ion would carry current according to its free solution concentration and mobility.

There is experimental data supporting and detracting from each of the candidates for current carrier. Proving the existence of a coupling conductance g_x and determining the current carrier through g_x are experimental problems that may have the same solution. Unfortunately, one must expect that identification of the mobile species will be impeded by the series connection of the T-SR junction and SR membranes, with the resulting complexity in selectivity and other properties.

Experimental Tests

It is useful to consider experiments that might distinguish between the movement of intramembrane charges and current flow from T system to SR. The experiments we have considered fall into three categories.

First, there are purely electrical experiments in which the response to multistep pulse schedules are evaluated. Consider an experiment in which the potential is changed from the holding potential to a depolarized potential (e.g., 0 mV) and then returned to a potential V_{return}. The passive model, with the parameters given in Tables I and II, predicts that the charge movement associated with the change of potential from 0 to V_{return} will increase as V_{return} is made more negative than the holding potential. An increase is not expected in models explaining the OFF transient as the movement of a membrane-bound charge. Such experiments may distinguish between the two models, but it may also be possible to modify the passive model to make the increase in charge movement rather small. In any case, experiments of this type will better specify the properties of g_x. The properties of charge movement—and, thus, of the circuit elements in our models—need to be investigated in the frequency domain. Measuring the impedance (and thus the equivalent circuit) of a muscle fiber at various holding potentials should specify the properties of charge movement in great detail and, thus, aid in distinguishing between models.

Another class of experiments we have considered might serve to falsify the class of models considered here. Models that involve ionic current flow from T system to SR, and that seek to explain all of charge movement as a consequence of that ionic current flow, seem to require substantial isolation of the longitudinal tubules from the terminal cisternae and seem to require that calcium release be electrically silent, as defined above. If it were found that calcium release is accompanied by a substantial net current, or that the longitudinal tubules were not isolated from the SR, it seems likely that the class of models considered here could not explain the charge movement measured in frog skeletal muscle.

The last class of experiments are designed to detect the movement of an extracellular substance into the SR. Unfortunately, a compartmental analysis of flux measurements seems unable to provide such a demonstration (Neville, 1979). But flux measurements might be able to detect the movement of a labeled impermeable solute, such as sucrose, from extracellular space into the

SR. Other experiments, which seek the penetration of an extracellular marker into the SR, appear promising. Endo (1966), Howell (1974), and probably Hill (1964), seem to have found extracellular markers in the terminal cisternae of the SR. Their findings are subject to other interpretations, however, and a decisive experiment demonstrating movement of an extracellular marker into the SR has not yet been performed.

APPENDIX

Linear and Nonlinear Effective Capacitance in Complex Tissues

This Appendix analyzes simple circuits (Fig. A 1) in which a voltage- and time-dependent conductance, in series with a membrane, produces transient currents resembling the intramembrane movement of charge called "gating current." Chandler et al. (1976*b*) considered similar circuits but with different properties for the conductance g_x. They concluded that circuits with those properties do not give equal

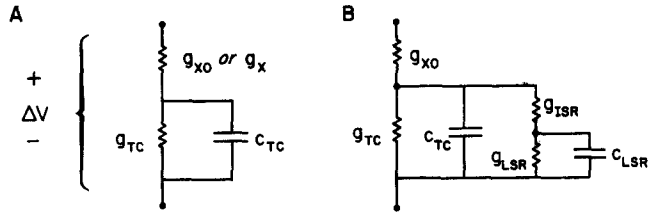

FIGURE A 1. Simple circuit models. *A* shows the "Linear" circuit model used to isolate the implications of g_x for measurements of transient currents. Note that the only voltage or time-dependent component in this circuit is g_x. *B* illustrates a more complex version of the linear circuit, which includes the longitudinal sarcoplasmic reticulum. The effective capacitance that these circuits contribute to a muscle fiber is computed in Eqs. A 4 and A 6.

charge movements at the ON and OFF of a depolarizing pulse. We shall show that such circuits can give approximately equal charge movements if they contain a series conductance with particular properties (Fig. A 2).

We consider charge movement defined by the following integral:

$$Q = \int_0^\infty \{i(t) - i(\infty)\}\, dt, \tag{A 1}$$

where Q is the total charge, $i(t)$ is the total current flowing through the circuit, and $i(\infty)$ is the steady state current flow. The difference $i(t) - i(\infty)$ is simply the transient current.

Our plan is to consider particular equivalent circuits (Fig. A 1) resembling those proposed for the T system and SR in the text of this paper. We analyze the circuit completely for the voltage-independent case, showing how all components can be determined from measurements of transients. Later, we show that a simple generalization of this circuit, with fixed capacitors and a single voltage- and time-dependent resistor, can give records quite similar to those of gating current. It also will be possible to provide analytical approximations for the nonlinear case. The approxi-

mations are interesting in themselves and useful in understanding the response of more complex circuits.

Our first step is to compute the response of the circuit (Fig. A 1, *A*) to-a step of potential ΔV, assuming that the circuit parameters are independent of voltage. Later we generalize the circuit to determine voltage-dependent transients comparable to gating current.

$$i(t) = -\Delta V \left\{ \frac{g_{xo} g_{TC}}{g_{TC} + g_{xo}} + \frac{g_{xo}^2}{g_{TC} + g_{xo}} \exp\left(-t \frac{g_{TC} + g_{xo}}{c_{TC}} \right) \right\} \qquad \text{(A 2)}$$

Three parameters are easily measurable from the transient response: the DC input conductance g_{eff}, the time constant τ, and the effective capacitance c_{eff}.[2] The effective

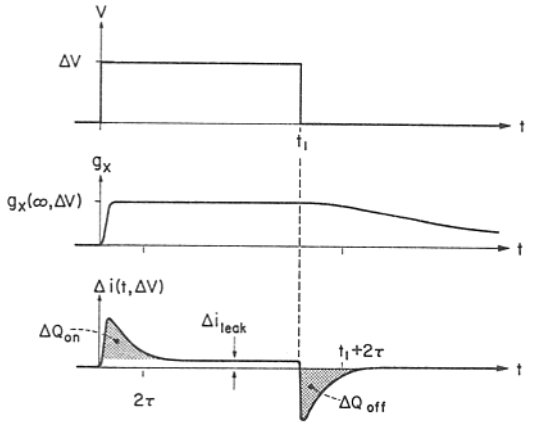

FIGURE A 2. The time dependence of the postulated conductance from T system to SR and the resulting transient current. The record labeled g_x shows the assumed time dependence following a depolarization of ΔV. The conductance g_x reaches a steady value called $g_x(\infty, \Delta V)$; for other values of ΔV, the time-course is almost identical but, of course, $g_x(t = \infty)$ changes. The nonlinear transient current, resulting from the addition of currents from depolarizing and hyperpolarizing pulses ΔV is shown as $\Delta i(t, \Delta V)$, with steady level of current Δi_{leak} determining the nonlinear leak conductance defined by $\Delta g_{eff} \equiv \Delta i_{leak}/\Delta V$. The integrals of the transient currents, indicated by stippled areas, determine the nonlinear charge movements ΔQ_{on} and ΔQ_{off}.

capacitance c_{eff} is defined as $Q/\Delta V$, where ΔV is the step of voltage applied to the terminals from which current is measured. These measurable parameters are related to the circuit components by the equations (Mathias, 1979):

$$g_{eff} = \frac{g_{xo} g_{TC}}{g_{xo} + g_{TC}} \qquad \tau = \frac{c_{TC}}{g_{xo} + g_{TC}}. \qquad \text{(A 3)}$$

[2] The choice of measured parameters is not unique, depending on whether current or voltage is applied to the circuit and on other practical matters. We choose these parameters because they can be determined with some ease and accuracy. The other obvious parameter is the current just after the step is applied, giving $g_{eff}(t = 0+)$; this parameter is difficult to determine, however, because of instrumentation errors most noticeable at short times.

In this circuit c_{eff} will be (see Eq. 13 A in the appendix by Adrian, Almers, and Chandler in Adrian and Almers, 1974, and the generalized results in Eisenberg and Mathias, 1980, Eqs. 10–12):

$$c_{\text{eff}} = \left(\frac{g_{xo}}{g_{xo} + g_{\text{TC}}}\right)^2 c_{\text{TC}}. \tag{A 4}$$

It is interesting that $\tau \neq c_{\text{eff}}/g_{\text{eff}}$. If this were not the case, the parameters defined in Eqs. A 3 and A 4 would not be independent and could not specify all the components in the circuit.

Note that the effective capacitance in this circuit, measured from the experimentally accessible terminals, does not equal the sum of the capacitors in the circuit. The effective capacitance depends on the attenuation factor $g_{xo}/(g_{xo} + g_{\text{TC}})$, indeed as much as on the capacitance. Changes in effective capacitance can be produced by changes in conductors as well as by changes in capacitors. The voltage across the inner membrane (labeled TC) is scaled, as one would expect, by the attenuation factor. But the component of the effective capacitance produced by the inner membrane is scaled by the square of the attenuation factor. For this reason, circuits of this morphology can have apparently paradoxical behavior. Voltages applied to the terminals can appear in large measure across the inner membranes, even though the capacitance of the inner membranes appears in small measure at the terminals. Consideration of the paths for current flow in this circuit resolves the paradox. The total charge deposited on c_{TC} depends on the voltage across c_{TC}, and this voltage is attenuated by $g_{xo}/(g_{xo} + g_{\text{TC}})$. But current flow measured at the outer terminals is only that fraction of the total current flow that flows through g_{xo}. Charge also redistributes by flowing from one plate of the capacitor c_{TC} to the other through g_{TC}. Thus, measured charge is less than the charge deposited on c_{TC}.

The circuit components shown in Fig. A 1 can be determined from the measured parameters by the following equations, determined by solving equations A 3 and A 4:

$$g_{xo} = g_{\text{eff}} + \frac{c_{\text{eff}}}{\tau} \qquad g_{\text{TC}} = g_{\text{eff}}\left(1 + \frac{\tau g_{\text{eff}}}{c_{\text{eff}}}\right)$$

$$c_{\text{TC}} = c_{\text{eff}} + 2\tau g_{\text{eff}} + \frac{g_{\text{eff}}^2 \tau^2}{c_{\text{eff}}}. \tag{A 5}$$

Fig. A 1 also shows a circuit with two stages of attenuation, closely related to the circuit models discussed in the body of this paper. The effective capacitance of this circuit is

$$c_{\text{eff}} = \left[\frac{g_{xo}}{g_{xo} + g_{\text{TC}} + \dfrac{g_{\text{ISR}} g_{\text{LSR}}}{g_{\text{ISR}} + g_{\text{LSR}}}}\right]^2 \left[c_{\text{TC}} + \left(\frac{g_{\text{ISR}}}{g_{\text{ISR}} + g_{\text{LSR}}}\right)^2 c_{\text{LSR}}\right]. \tag{A 6}$$

Note that the capacitance of the innermost membrane (called LSR) is multiplied by the squares of two attenuation factors. The contribution of the innermost membrane capacitor to the effective capacitance is much less than the value of that capacitor.

Voltage-dependent Case

The previous analysis of the voltage-independent case does not directly apply to a general voltage- and time-dependent circuit. But the analysis does describe a relevant

class of voltage- and time-dependent circuits. For that class of circuits, we derive analytical approximations for the linear and nonlinear effective conductance and charge movement after a step depolarization of ΔV and the subsequent repolarization to resting potential.

We consider a particular voltage-dependent case in which g_x changes rapidly soon after a depolarization and slowly after repolarization (Fig. A 2). We assume that, after a depolarization, g_x reaches its steady value rapidly, before there has been much ON charge movement. We further assume that, after repolarization, g_x remains at its depolarized value during most of the OFF charge movement, returning to its resting value only after most of the charge movement is complete.

In this situation, g_x during the ON is defined by Eq. 1 with $\xi_x \equiv 1$, and with $\Delta V = V_w - E_x$. The variable $N_x(\Delta V)$ is shown in Fig. 3 C. Then, the value of Q_{on} can be estimated from Eq. A 4, with $g_x(\infty, \Delta V)$ replacing g_{xo}. The value of Q_{off} upon repolarization can be estimated by a similar procedure if g_x is supposed to change slowly in that case. In more formal language, we assume that, for times between t_1 (when the repolarization is applied) and $t_1 + 2\tau$, the conductance $g_x(t - t_1) \simeq g_x(\infty, \Delta V)$. Then, we have for the simple circuit in Fig. A 1,

$$Q_{on} \simeq Q_{off} \simeq \Delta V \left(\frac{g_x(\infty, \Delta V)}{g_x(\infty, \Delta V) + g_{TC}} \right)^2 c_{TC}. \tag{A 7}$$

This demonstrates that the transient currents occurring in this class of voltage-dependent circuits will have one of the properties of nonlinear polarization current, approximate equality of ON and OFF charge movement, even though the circuit is devoid of nonlinear capacitors. Note that we have made no requirements on the relative values of the series conductance g_x, the membrane conductance g_{TC}, or the capacitance c_{TC}. Even if a large fraction of the charge deposited on c_{TC} flows through g_{TC}, the transient currents measured from the outer terminals will still show equal ON and OFF areas and so will share one of the characteristics of polarization currents. Eq. A 7 only requires that $g_x(t, \Delta V)$ have a particular time-course. Indeed, even this requirement can be relaxed if restrictions are placed on the relative value of the conductances. In the special case that the conductance g_x is much larger than g_{TC} for most of the time after a depolarization and for most of the time after a repolarization (see Fig. A 2), then $Q_{on} \simeq Q_{off}$ for a wide variety of time courses of g_x. There may well be other situations, for example, involving correlated properties of g_x and g_{TC}, in which ON and OFF charge movements are approximately equal.

Having established that transient currents produced by voltage-dependent resistors can mimic polarization currents, we now examine these transient currents in more detail (Fig. A 3). Suppose that we add the currents measured from depolarizing and hyperpolarizing steps, according to the paradigm used to identify gating currents. Note that in these computations the circuit elements are considered essentially constant at voltages more negative than the resting potential. The results of the addition process are marked with a delta. Because $g_x(\infty, \Delta V) > g_{xo}$, the charge movement for depolarizing steps Q_{on} is larger than its counterpart during the hyperpolarizing step used to estimate linear currents. The addition procedure shows the increment in the movement of polarization charge with depolarization:

$$\Delta Q = \Delta V c_{TC} \left[\left(\frac{g_x(\infty, \Delta V)}{g_x(\infty, \Delta V) + g_{TC}} \right)^2 - \left(\frac{g_{xo}}{g_{xo} + g_{TC}} \right)^2 \right]. \tag{A 8}$$

Necessarily associated with the increment in g_x (used to obtain asymmetrical charge

movement) is an increment in the measured conductance:

$$\Delta g_{\text{eff}} = \frac{g_{\text{TC}} g_x(\infty, \Delta V)}{g_x(\infty, \Delta V) + g_{\text{TC}}} - \frac{g_{xo} g_{\text{TC}}}{g_{xo} + g_{\text{TC}}} \tag{A 9}$$

Eqs. A 8 and A 9 specify the amount of nonlinear charge movement and nonlinear "leak" current in terms of the voltage dependence of g_x. (Eqs. A 2 and A 3 can be used to determine the effect on the time-course of the nonlinear charge movement).

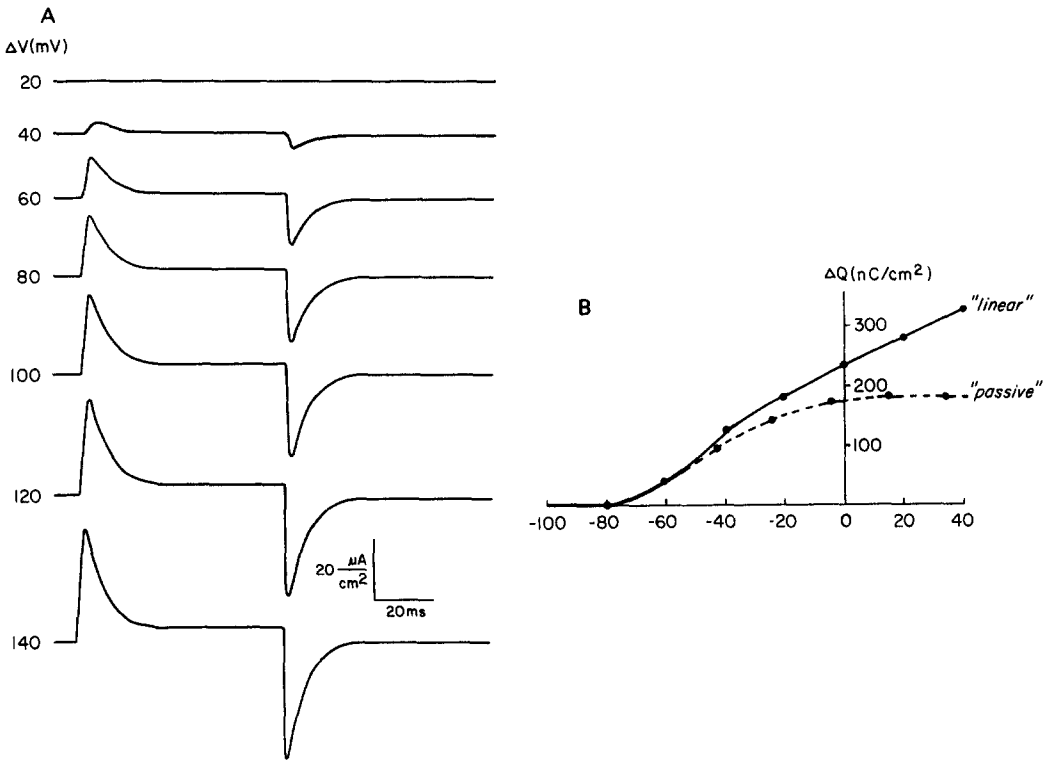

FIGURE A 3. The asymmetry currents produced by the linear model. *A* shows the nonlinear currents produced for a set of ΔV's. Note that each record is the sum of the currents produced by a depolarizing and hyperpolarizing pulse. *B* shows the integrals of the transient charge (i.e., the stippled area of Fig. A 2) for both linear and passive models. The latter results are shown in more detail in Fig. 4.

The conductances g_x and g_{TC} influence the amount of nonlinear charge and nonlinear ionic current in different ways. Here, increasing the amount of g_x present at depolarized potentials increases the amount of nonlinear charge and nonlinear ionic current. Conversely, we could have chosen to decrease g_{TC} with depolarization. That choice would most likely have increased c_{eff} while decreasing Δg_{eff}.

The time-courses of the responses shown in Fig. A 3 are determined by Eq. A 2 with parameters calculated using Eqs. A 3–A 5 from the values specified, for the most part, in Tables I and II. However, in the calculations illustrated in Fig. A 3: (*a*) the

parameters g_x and g_{TC} are not given instantaneous rectification; (*b*) the turn off rate of g_x is slower than in the text of the paper, i.e., here a_{min} is 80 s^{-1}; (*c*) ΔV in the calculation is analogous to $V_w - E_x$ in the text.

The derived quantity ΔQ is shown in Fig. A 3. As ΔV increases, $g_x(\infty, \Delta V)$ increases, and ΔQ increases more steeply than linearly. As ΔV increases further, $g_x(\infty, \Delta V)$ saturates, and ΔQ continues to increase but at a lesser slope. Thus, the curve relating ΔQ and ΔV bends but does not saturate. This result differs from the saturating behavior expected from a true intramembrane charge movement. A more complex model, called the passive model, is introduced in the body of the paper and produces saturation by making the voltage across c_{TC} saturate at large depolarizations. Nonetheless, even the simple circuit produces nonlinear charge movement qualitatively similar to that measured in frog skeletal muscle.

The computations shown in Fig. A 3 were done, of course, with parameters chosen to ensure this similarity with experimental data from frog skeletal muscle. In effect, the computations use effective parameters similar to those measured experimentally. But the values of the circuit components are not arbitrary. Once the theory is matched to the experimental data, the circuit components are determined. Because the circuit components are supposed to describe the properties of experimentally known amounts of real structures within the muscle, the values of the circuit components must reasonably correspond to the likely properties of those structures, if the model is to be acceptable. The values of the circuit elements describing membranes in the legend of Fig. A 1 are consistent with the area and likely specific capacitance of the membranes of terminal cisternae. The figure for the conductance g_x is much less than that expected for a gap junction, if one assumes that all sites identified by Franzini-Armstrong (1970) contain functional gap junctions. A value of g_x larger than that for gap junctions would have seemed inconsistent with the impermeability of the T–SR junction to large molecules.

We conclude from this example that in tissues of complex geometry the presence of nonlinear transient current, which shows approximate equality of ON and OFF charge movements, can be explained in at least two ways: as a capacitive current induced by an intramembrane charge movement analagous to gating current, or, as a transient current controlled by a voltage-dependent conductor in series with a fixed membrane capacitance.

We have stressed the implications of complex morphology in the analysis of nonlinear charge movement. Even simple preparations, however, are described by *A* of Fig. A 1, with, perhaps, a voltage-dependent membrane conductance g_{TC}. That circuit can mimic the qualitative properties of gating current, even with a voltage-independent capacitance, if the series resistance is voltage dependent, and perhaps otherwise as well.

Dr. B. Eisenberg has informed and reminded us of the structural aspects of excitation-contraction coupling. We are grateful to her, Dr. M. Neville, Dr. J. Rae, and Dr. C. Schauf for their critical reading of the manuscript.

The work was supported by grants from the Muscular Dystrophy Association and the National Institutes of Health (HL 20230).

Received for publication 30 August 1979.

REFERENCES

ADRIAN, R. H. 1964. The rubidium and potassium permeability of frog muscle membrane. *J. Physiol. (Lond.)*. **175:**134–159.

ADRIAN, R. H. 1978. Charge movement in the membrane of striated muscle. *Annu. Rev. Biophys. Bioeng.* **7**:85–112.

ADRIAN, R. H., and W. ALMERS. 1974. Membrane capacity measurements on frog skeletal muscle in media of low ion content. *J. Physiol. (Lond.)*. **237**:537–605.

ADRIAN, R. H., and W. ALMERS. 1976 *a*. The voltage dependence of membrane capacity. *J. Physiol. (Lond.)*. **254**:317–338.

ADRIAN, R. H., and W. ALMERS. 1976 *b*. Charge movement in the membrane of striated muscle. *J. Physiol. (Lond.)*. **254**:339–360.

ADRIAN, R. H., and L. D. PEACHEY. 1973. Reconstruction of the action potential of frog sartorius muscle. *J. Physiol. (Lond.)*. **235**:103–131.

ADRIAN, R. H., and A. PERES. 1977. A gating signal for the potassium channel? *Nature (Lond.)*. **267**:800–804.

ADRIAN, R. H., and A. PERES. 1979. Charge movement and membrane capacity in frog muscle. *J. Physiol. (Lond.)* **289**:83–97.

ADRIAN, R. H., and R. F. RAKOWSKI. 1978. Reactivation of membrane charge movement and delayed potassium conductance in skeletal muscle fibres. *J. Physiol. (Lond.)*. **278**:533–557.

ADRIAN, R. H., W. K. CHANDLER, and A. L. HODGKIN. 1969. The kinetics of mechanical activation in frog muscle. *J. Physiol. (Lond.)*. **204**:207–230.

ADRIAN, R. H., W. K. CHANDLER, and A. L. HODGKIN. 1970 *a*. Voltage clamp experiments in striated muscle fibers. *J. Physiol. (Lond.)*. **208**:607–644.

ADRIAN, R. H., W. K. CHANDLER, and A. L. HODGKIN. 1970 *b*. Slow changes in potassium permeability in skeletal muscle. *J. Physiol. (Lond.)*. **208**:645–668.

ADRIAN, R. H., W. K. CHANDLER, and R. F. RAKOWSKI. 1976. Charge movement and mechanical repriming in skeletal muscle. *J. Physiol. (Lond.)*. **254**:361–388.

ALMERS, W. 1978. Gating currents and charge movements in excitable membranes. *Rev. Physiol. Biochem. Pharmacol.* **82**:96–190.

ALMERS, W., and P. M. BEST. 1976. Effects of tetracaine on displacement currents and contraction of frog skeletal muscle. *J. Physiol. (Lond.)*. **262**:583–611.

ARMSTRONG, C. M., and F. BEZANILLA. 1974. Charge movement associated with the opening and closing of the activation gates of the Na channels. *J. Gen. Physiol.* **65**:533–552.

ARMSTRONG, C. M., and F. BEZANILLA. 1977. Inactivation of the sodium channel. II. Gating current experiments. *J. Gen. Physiol.* **70**:567–590.

BAYLOR, S. M., and H. OETLIKER. 1977. A large birefringence signal preceding contraction in single twitch fibres of the frog. *J. Physiol. (Lond.)*. **264**:141–162.

BAYLOR, S. M., W. K. CHANDLER, and M. W. MARSHALL. 1979. Temporal comparison of optical signals associated with E-C coupling in frog muscle. *Biophys. J.* **25**:119 *a*. (*Abstr.*).

BEZANILLA, F., and P. HOROWICZ. 1975. Fluorescence intensity changes associated with contractile activation in frog muscle stained with Nile blue A. *J. Physiol. (Lond.)*. **246**:709–735.

BIANCHI, C. P., and A. M. SHANES. 1959. Calcium influx in skeletal muscle at rest, during activity, and during potassium contracture. *J. Gen. Physiol.* **42**:803–815.

BIRKS, R. I. 1965. The sarcoplasmic reticulum of twitch fibers in the frog sartorius muscle. *In* Muscle. W. M. Paul, E. E. David, C. M. Kay, and G. Monckton, editors. Pergamon Press Ltd., Oxford. 199–216.

CAPUTO, C. 1978. Excitation and contraction processes in muscle. *Annu. Rev. Biophys. Bioeng.* **7**: 63–83.

CHANDLER, W. K., and M. F. SCHNEIDER. 1976. Time-course of potential spread along a skeletal fiber under voltage clamp. *J. Gen. Physiol.* **67**:165–184.

CHANDLER, W. K., R. F. RAKOWSKI, and M. F. SCHNEIDER. 1976 *a*. A non-linear voltage dependent charge movement in frog skeletal muscle. *J. Physiol. (Lond.)*. **254**:245–283.

CHANDLER, W. K., R. F. RAKWOSKI, and M. F. SCHNEIDER. 1976 *b*. Effects of glycerol treatment and maintained depolarization on charge movement in skeletal muscle. *J. Physiol. (Lond.)*. **254:**285–316.

COSTANTIN, L. L. 1975. Contractile activation in skeletal muscle. *Prog. Biophys. Mol. Biol.* **29:** 197–224.

COSTANTIN, L. L., and S. R. TAYLOR. 1973. Graded activation in frog muscle fibers. *J. Gen. Physiol.* **61:**424–443.

COSTANTIN, L. L., C. FRANZINI-ARMSTRONG, and R. J. PODOLSKY. 1965. Localization of calcium-accumulating structures in striated muscle fibers. *Science (Wash. D. C.)*. **147:**158–160.

EISENBERG, B. R., and A. GILAI. 1979. Structural changes in single muscle fibers after stimulation at a low frequency. *J. Gen. Physiol.* **74:**1–16.

EISENBERG, B. R., R. S. EISENBERG, and A. GILAI. 1979. Structural changes in the T-SR junction in actively contracting skeletal muscle. *Biophys. J.* **25:**118 *a*. *(Abstr.)*.

EISENBERG, B. R., R. T. MATHIAS, and A. GILAI. 1979. The intracellular localization of peroxidase within frog muscle fibers. *Am. J. Physiol.* **237:**C50–C55.

EISENBERG, R. S., and R. T. MATHIAS. 1980. Structural analysis of electrical properties of cells and tissues. *Crit. Rev. Bioeng.* In press.

ENDO, M. 1966. Entry of fluorescent dyes into the sarcotubular system of the frog muscle. *J. Physiol. (Lond.)*. **185:**224–238.

ENDO, M. 1977. Calcium release from the sarcoplasmic reticulum. *Physiol. Rev.* **57:**71–108.

FORD, L. E., and R. J. PODOLSKY. 1972. Intracellular calcium movements in skinned muscle fibers. *J. Physiol. (Lond.)*. **223:**21–33.

FRANZINI-ARMSTRONG, C. 1970. Studies of the triad. I. Structure of the junction in frog twitch fibers. *J. Cell Biol.* **47:**488–499.

FRANZINI-ARMSTRONG, C. 1971. Studies of the triad. II. Penetration of tracers into the junctional gap. *J. Cell. Biol.* **49:**196–203.

FRANZINI-ARMSTRONG, C. 1974. Freeze fracture of skeletal muscle from the tarantula spider. *J. Cell Biol.* **61:**501–513.

FRANZINI-AMSTRONG, C., and K. R. PORTER. 1964. Sarcolemmal invaginations constituting the T system in fish muscle fibers. *J. Cell Biol.* **22:**675–696.

FREYGANG, W. H. 1965. Tubular ionic movements. *Fed. Proc.* **24:**1135–1140.

HILL, D. K. 1964. The space accessible to albumin within the striated muscle fiber of the toad. *J. Physiol. (Lond.)*. **175:**275–295.

HODGKIN, A. L., and P. HOROWICZ. 1960. The effect of sudden changes in ionic concentrations on the membrane potential of single muscle fibers. *J. Physiol. (Lond.)*. **153:**370–385.

HODGKIN, A. L., and A. F. HUXLEY. 1952. A quantitative description of membrane current and its application to conduction and excitation in nerve. *J. Physiol. (Lond.)*. **117:**500–544.

HODGKIN, A. L., and S. NAKAJIMA. 1972 *a*. The effect of diameter on the electrical constants of frog skeletal muscle fibers. *J. Physiol. (Lond.)*. **221:**105–120.

HODGKIN, A. L., and S. NAKAJIMA. 1972 *b*. Analysis of the membrane capacity in frog muscle. *J. Physiol. (Lond.)*. **221:**121–136.

HOWELL, J. N. 1974. Intracellular binding of ruthenium red in frog skeletal muscle. *J. Cell Biol.* **62:**242–247.

HUXLEY, A. F., and R. E. TAYLOR. 1958. Local activation of striated muscle fibers. *J. Physiol. (Lond.)*. **144:**426–441.

HUXLEY, A. F. 1971. The activation of striated muscle and its mechanical response. *Proc. R. Soc. Lond. B Biol. Sci.* **178:**1–27.

KAO, C. Y., and P. R. STANFIELD. 1968. Actions of some anions on electrical properties and mechanical threshold of frog twitch muscle. *J. Physiol. (Lond.)*. **198:**291–309.

KAO, C. Y., and P. R. STANFIELD. 1970. Actions of some cations on the electrical properties and mechanical threshold of frog sartorius muscle fibers. *J. Gen. Physiol.* **55:**620–639.

KELLY, D. E., and A. M. KUDA. 1979. Subunits of the triadic junction in fast skeletal muscle as revealed by freeze-fracture. *J. Ultrastruct. Res.* **68:**220–233.

KEYNES, R. D., and E. ROJAS. 1974. Kinetics and steady-state properties of the charged system controlling sodium conductance in the squid giant axon. *J. Physiol. (Lond.).* **239:**393–434.

KIRBY, A. C., B. D. LINDLEY, and J. R. PICKEN. 1975. Calcium content and exchange in frog skeletal muscle. *J. Physiol. (Lond.).* **253:**37–52.

KOVACS, L., E. RIOS, and M. F. SCHNEIDER. 1979. Calcium transients and intramembrane charge movement in skeletal muscle fibers. *Nature (Lond.).* **279:** 391–396.

LÜTTGAU, H. C., and G. D. MOISESCU. 1978. Ion movements in skeletal muscle in relation to the activation of contraction. *In* Physiology of Membrane Disorders. T. Audreoli, editor. Plenum Press, New York. 493–515.

LÜTTGAU, H. C., and W. SPIECKER. 1979. The effects of calcium deprivation upon mechanical and electrophysiological parameters in skeletal muscle fibers of the frog. *J. Physiol. (Lond.).* **296:**411–429.

MATHIAS, R. T. 1979. An analysis of the consequence of electrical continuity between the T-system and sarcoplasmic reticulum. *J. Physiol. (Lond.).* **288:** 65–68.

MOBLEY, B. A., and B. EISENBERG. 1975. Sizes of components in frog skeletal muscle measured by methods of stereology. *J. Gen. Physiol.* **66:**31–45.

MORAD, M., and Y. GOLDMAN. 1973. Excitation-contraction coupling in heart muscle; membrane control of development of tension. *Prog. Biophys. Mol. Biol.* **27:**257–313.

NEVILLE, M. C. 1979. The extracellular compartments of frog skeletal muscle. *J. Physiol. (Lond.).* **288:**45–70.

PALADE, P. T., and W. ALMERS. 1978. Slow Na and Ca currents across the membrane of frog skeletal muscle fibers. *Biophys. J.* **21:**18 *a.* (*Abstr.*).

PEACHEY, L. D. 1965 *a.* The sarcoplasmic reticulum and transverse tubules of the frog's sartorius. *J. Cell Biol.* **25** (3, Pt. 2):209–231.

PEACHEY, L. D. 1965 *b.* Structure of the sarcoplasmic reticulum and T-system of striated muscle. Proceedings of the XXIIIrd International Congress of Physiological Sciences. **87:**388–398.

PEACHEY, L. D. 1968. Muscle. *Annu. Rev. Physiol.* **30:**401–440.

PEACHEY, L. D., and K. R. PORTER. 1959. Intracellular impulse conduction in muscle cells. *Science (Wash. D. C.).* **129:**721–722.

PORTER, K. R., and C. FRANZINI-ARMSTRONG. 1965. The sarcoplasmic reticulum. *Sci. Am.* **212:** 73–80.

RAKOWSKI, R. F. 1978 *a.* Recovery of linear capacitance in skeletal muscle fibers. *Biophys. J.* **21:** 167 *a.* (*Abstr.*).

RAKOWSKI, R. F. 1978 *b.* Reprimed charge movement in skeletal muscle fibers. *J. Physiol. (Lond.).* **281:**339–358.

SANCHEZ, J. A., and E. STEFANI. 1978. Inward calcium current in twitch muscle fibres of the frog. *J. Physiol. (Lond.).* **283:**197–209.

SCHNEIDER, M. F., and W. K. CHANDLER. 1973. Voltage dependent charge movement in skeletal muscle: a possible step in excitation-contraction coupling. *Nature (Lond.).* **242:**244–246.

SCHNEIDER, M. F., and W. K. CHANDLER. 1976. Effects of membrane potential on the capacitance of skeletal muscle fibers. *J. Gen. Physiol.* **67:**125–163.

SOMMER, J. R., N. R. WALLACE, and W. HASSELBACH. 1978. The collapse of the sarcoplasmic reticulum in skeletal muscle. *Z. Naturforsch. Sect. C Biosci.* **33:**561–573.

SOMLYO, A. V. 1979. Bridging structures spanning the gap at the triad of skeletal muscle. *J. Cell Biol.* **80:**743–750.

SOMLYO, A. V., H. SHUMAN, and A. P. SOMLYO. 1977. Elemental distribution in striated muscle and the effects of hypertonicity. *J. Cell Biol.* **74:**828–857.

SPIECKER, W., W. MELZER, and H. C. LÜTTGAU. 1979. Extracellular Ca^{++} and excitation-contraction coupling. *Nature (Lond.)*. **280:**158–160.

STEPHENSON, E. W. 1978. Properties of chloride-stimulated ^{45}Ca flux in skinned muscle fibers. *J. Gen. Physiol.* **71:**411–430.

VALDIOSERA, R., C. CLAUSEN, and R. S. EISENBERG. 1974. Impedance of frog skeletal muscle fibers in various solutions. *J. Gen. Physiol.* **63:**460–491.

VERGARA, J., F. BEZANILLA, and B. M. SALZBERG. 1978. Nile blue fluorescence signals from cut single muscle fibers under voltage or current clamp conditions. *J. Gen. Physiol.* **72:**775–800.

WINEGRAD, S. 1968. Intracellular calcium movements of frog skeletal muscle during recovery from tetanus. *J. Gen. Physiol.* **51:**65–83.

WINEGRAD, S. 1970. The intracellular site of calcium activation of contraction in frog skeletal muscle. *J. Gen. Physiol.* **55:**77–88.